EXERGOECONOMIC ANALYSIS OF A SOLAR ASSISTED ORGANIC RANKINE CYCLE: CASE STUDY OF MARDIN, TURKEY

Fatih ÜNAL[1*], Merve Şentürk ACAR[2]

*[1] Mersin University, Engineering Faculty, Mechanical Engineering Department, Mersin, Türkiye

[2] Bilecik Seyh Edebali University, Engineering Faculty, Mechanical Engineering Department, Türkiye

*Corresponding author; E-mail: fatihunal@mersin.edu.tr

Escalating concerns over dwindling energy resources and environmental issues from unsustainable use and external energy dependence highlight the need to optimize existing energy sources. Harnessing renewable energy is crucial for minimizing environmental impact and reducing reliance on external suppliers. Integrating renewable energy technologies into existing systems offers a promising path to sustainable and efficient energy use. This study presents a solar-assisted organic Rankine cycle system designed for Mardin Province, based on long-term solar radiation data. The system uses parabolic collectors to capture solar thermal energy, stored using Therminol VP-1. This stored energy drives the organic Rankine cycle system throughout the day, using R-365mfc as the working fluid. The study integrates exergy and economic analyses to evaluate the system's performance and cost-effectiveness, providing a framework for similar renewable energy systems. The solar-assisted organic Rankine cycle system is designed to harness solar energy efficiently, contributing to sustainable energy solutions in high solar potential regions like Mardin Province. Extensive data analysis evaluates the system's energy, exergy, and exergoeconomic performance, and determines optimal turbine inlet and condenser pressures. The system's net power output ranges from 29.927 kW to 201.597 kW, with efficiencies from 3.74% to 16.079% and exergy efficiencies from 4.627% to 18.977%. These results confirm the system's suitability for sustainable energy generation in Mardin Province.

Key Words*: solar energy, Rankine cycle, solar assisted organic Rankine cycle, thermodynamic analysis, exergy analysis, exergoeconomic analysis*

1. Introduction

In recent years, the surge in industrialization driven by rapid population growth has significantly escalated the energy demand, primarily met by the utilization of fossil fuels. However, the consequential environmental degradation and the looming specter of fossil fuel depletion within the foreseeable future have propelled a notable shift towards embracing environmentally sustainable renewable energy sources. This transition is evident in the burgeoning popularity of solar energy, geothermal energy, wind energy, and ocean energy, all of which are witnessing increasing trends. Turkey stands out as geographically endowed with abundant renewable energy resources, positioning

the nation favorably in the global transition toward sustainability. The country's exceptional solar energy potential, in particular, has spurred extensive research and development efforts in this domain. Today, amidst the backdrop of finite energy resources and the compounding economic and environmental challenges stemming from their indiscriminate exploitation, there exists an imperative to optimize the utilization of available energy reservoirs. To address these pressing concerns, the integration of renewable energy technologies into existing energy systems emerges as a paramount strategy. This integration not only fosters sustainable energy practices but also enhances energy efficiency, thus aligning with broader environmental and economic objectives. Recent advancements in renewable energy technologies have significantly improved the efficiency and economic viability of various energy systems. This study focuses on the integration of solar-assisted Organic Rankine Cycles (S-ORCs), a promising technology for harnessing solar energy. The state of the art in this field highlights several key developments and research findings. The literature abounds with various studies exploring the viability and efficacy of solar-assisted Organic Rankine Cycle (S-ORC) systems, reflecting the concerted efforts towards leveraging renewable energy sources to mitigate the multifaceted challenges associated with energy consumption. Bou Lawz Ksayer conducted a study on solar Rankine cycles aimed at generating hot water and electricity for conventional residences. They employed R245fa as the working fluid and reported an overall efficiency of 14.35% during sunny hours and 9.6% during non-sunny hours (morning, evening, and night) [1]. Yamaguchi and colleagues introduced a solar Rankine cycle concept featuring the utilization of supercritical CO_2 for the simultaneous generation of electricity and thermal energy. Their system design incorporated several key components, including vacuum tube solar collectors, a power-generating turbine, high-temperature heat recovery mechanisms, low-temperature heat recovery components, and a feed pump. Through experimental investigations, they demonstrated the system's capability for stable operation within a non-critical region, showcasing the viability and potential of employing CO_2-based solar Rankine cycles for efficient energy production [2]. Ango et al. focused their study on the design and testing of a 3 kW radial turbine. Laboratory tests showed an isentropic efficiency of around 40% and a cycle efficiency of around 5%. Their research showed that the S-ORC system, heated at medium temperatures and combined with thermal energy storage (TES), is a promising approach for decentralized and sustainable cogeneration [3]. Li et al. introduced a novel hybrid energy generation system that integrates a Solid Oxide Fuel Cell (SOFC), an Internal Combustion Engine (ICE), and an Organic Rankine Cycle (ORC). The system, which uses methanol as its fuel source, underwent thorough analyses in terms of energy, exergy, and exergoeconomic. Their research provides significant insights into optimizing hybrid power systems for sustainable energy applications [4]. Wang et al. designed a low-temperature solar-powered Rankine cycle employing R245fa as the working fluid. Their experimental setup incorporated a vacuum tube collector, a flat collector, and a rotary piston expander. They reported an average power output of 1.73 kW and an average isentropic efficiency of 45.2%, affirming the feasibility of R245fa in low-temperature solar energy Rankine cycles [5]. Desai and associates integrated a parabolic slotted collector with the Rankine cycle, investigating the impact of turbine inlet pressure and temperature variations, design irradiance, plant size, and Rankine cycle on average efficiency. They determined that the turbine inlet pressure range for a 1 MW plant is approximately 3.5–7.5 Mpa [6]. Zhu and Huang combined a collector with the ORC, exploring various configurations including single-stage and two-stage setups. They utilized R245fa and R134a as working fluids, concluding that the two-stage ORC yields higher efficiency than the single-stage when

using R245fa. Conversely, with R134a, the two-stage ORC exhibited lower efficiency compared to the single-stage counterpart [7]. Mitrovic et al. conducted a detailed exergy and exergoeconomic analysis to identify and quantify the sources and magnitudes of irreversibility within the steam boiler and other components in a 348.5 MW thermal power plant. Their findings highlight the critical areas for efficiency improvements and cost reductions in thermal power plant operations [8]. Marques et al. presented a detailed thermo-economic analysis of a micro CHP unit with an internal combustion engine and a single-effect NH3-water absorption chiller. The Theory of Exergetic Cost method was used to evaluate both monetary and energy costs, as well as exergy efficiency, to identify areas for improvement within the energy system [9]. Unal and his colleagues have extensively utilized energy, exergy, and exergoeconomic analysis in their research on power plants, thermal systems, and solar-assisted hybrid systems. Their various studies have focused on optimizing system performance and identifying opportunities for cost reduction. By applying these comprehensive analytical methods, they have been able to pinpoint inefficiencies and suggest improvements that enhance both economic and environmental sustainability [10-14]. Boydak et al. examined the utilization of resources in generating electricity through power turbine cycles. Despite the advantages of compact design and cost-effectiveness, they highlighted a persistent challenge with thermal efficiency in low-temperature Rankine cycles. They proposed the ORC, which employs organic fluids with boiling points lower than water, as a viable solution. Nevertheless, they observed that its efficiency is typically 10% to 20%, influenced by the temperature conditions and the availability of the working fluid [15]. Gao et al. studied a seasonal solar combined cooling, heating, and power (CCHP) system using evacuated flat plate collectors and an ORC. They noted that the system they examined used heat collected by collectors to power an ORC unit during the cool seasons and a double-effect lithium bromide absorption chiller during the summer months. They observed that system performance varies between locations [16]. Zhao et al. addressed the challenge of selecting the most suitable ternary refrigerants for cooling systems by proposing a mechanism model in their study. In the model, they applied to an ORC-VCR-CCHP system for university campuses for energy demands aimed to simultaneously optimize the refrigerant composition and process parameters. In the model they used, they prioritized exergoeconomic efficiency while ensuring economy, environmental friendliness, thermodynamic stability, and low toxicity. They stated that the optimization results showed a peak exergoeconomic efficiency of 42.49% by the optimum compositions determined for the ORC and VCR systems [17]. Quoilin et al. focused on designing an ORC tailored for electricity generation in rural Lesotho. Their system comprised a small-scale ORC, a parabolic collector, and a storage tank. They developed a model facilitating component sizing, performance evaluation, comparison of working fluids, and simulation of single and double-stage configurations [18].

In this study, a departure from the conventional Rankine cycle for electricity generation was made by integrating the working fluid with parabolic collectors, utilizing the high molecular R 365 mfc fluid, which boasts a lower boiling point compared to water. Within this framework, the S-ORC was meticulously designed, drawing upon long-term solar radiation data specific to Mardin Province. This investigation presents a novel S-ORC designed to operate in Mardin Province, leveraging its specific solar radiation profile. The system continuously supplies thermal energy to the ORC throughout the day via a dedicated thermal energy storage (TES) unit. Parabolic collectors efficiently capture solar radiation, transferring the collected heat to the TES system, where Therminol VP-1 acts as the working fluid. This stored thermal energy then drives the ORC cycle, utilizing R-365mfc as the

working fluid. Notably, this research distinguishes itself from prior studies by meticulously tailoring the system design to the unique solar radiation characteristics of Mardin Province. Furthermore, the study employs a comprehensive analytical approach, encompassing energy, exergy, and exergoeconomic analyses of the entire system and its components. This multi-faceted approach aims to provide a profound understanding of the system's performance and economic viability, ultimately assessing its suitability for energy generation in Mardin Province. This study is expected to make significant contributions to the field of renewable energy systems by providing a comprehensive framework for the exergoeconomic analysis of S-ORCs. The application of this analysis to a case study in Mardin, Turkey, offers valuable insights into the practical benefits and feasibility of such systems in similar climates. The methodological advancements presented in this study enhance the accuracy of performance evaluations, leading to important implications that support informed decision-making in energy policy for policymakers and planners. Furthermore, the study identifies future research directions, such as the optimization of system components and integration with other renewable resources, paving the way for further advancements in renewable energy technologies.

2. Material and Method

The methodology used in this study follows a structured approach, starting with problem definition, where the research problem and objectives are identified, and the scope and limitations are defined. A comprehensive literature review is carried out to understand the current research on S-ORC systems and identify research gaps. The system design and modeling phase involves the design of the S-ORC system, the development of a detailed model using appropriate software tools, and the definition of system parameters and assumptions. Relevant data specific to the case study location (Mardin, Turkey) were collected, including weather data, solar radiation data, and economic data. The exergoeconomic analysis integrates energy and exergy analysis, which evaluates thermodynamic performance, and economic analysis, which assesses cost-effectiveness, to provide a comprehensive assessment of the system's performance. The results from the exergoeconomic analysis were then analyzed and compared with existing literature, and the discussion highlighted the practical applications and policy implications of the findings. Finally, the study concludes with a summary of key findings and recommendations for future research and practical implementation, ensuring that the research contributes to the advancement of knowledge and provides guidance for further studies. The flow chart of the study is given in Fig. 1.

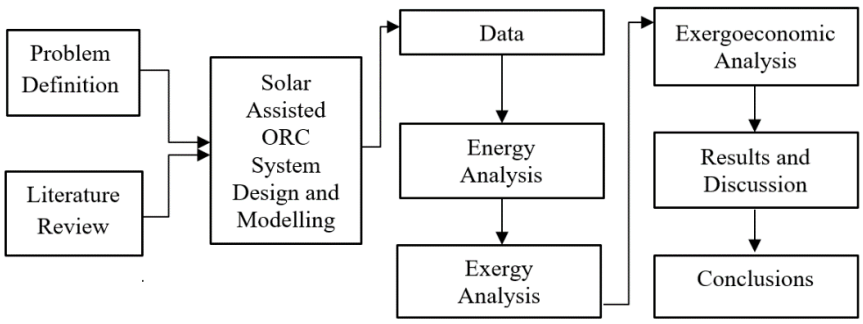

Figure 1. The flow chart of the methodology

In the system tailored for Mardin Province, a thermal energy storage tank (TES) serves as a pivotal component for integrating solar energy into the ORC. The primary objective is to ensure a continuous energy supply to the ORC by storing the solar energy accumulated during daylight hours within the TES. This strategic utilization of thermal energy storage enhances the system's resilience to fluctuations in solar radiation and enables sustained operation beyond daylight periods. Therminol VP-1 has been specifically chosen as the working fluid within the TES, offering optimal thermal properties and efficiency for the storage and retrieval of solar-derived thermal energy. This integrated approach not only maximizes the utilization of renewable solar resources but also enhances the overall effectiveness and reliability of the ORC system tailored to the unique conditions of Mardin Province. Fig. 2 presents a flow diagram of the S-ORC. A Thermal Energy Storage (TES) tank plays a crucial role, integrating solar energy captured during the day and providing continuous power to the ORC throughout the day. Therminol serves as the working fluid in the parabolic collectors, transferring heat to molten salt stored within the TES. This heated salt then circulates through a heat exchanger, efficiently transferring its thermal energy to the ORC's dedicated working fluid. Finally, the ORC's working fluid expands in the turbine, generating electricity.

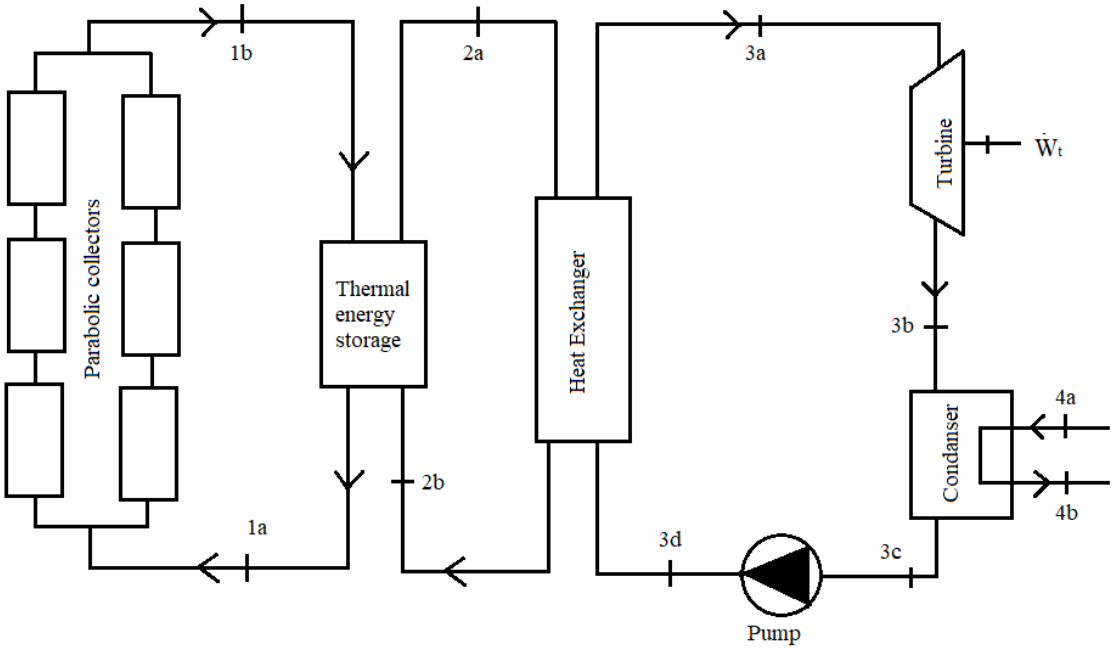

Figure 2. The flow diagram of the S-ORC

R-365mfc was chosen as the working fluid for the S-ORC system. Its thermodynamic properties were obtained using REFPROP software [19]. The design incorporates various turbine inlet pressures and temperatures based on the chosen fluid's specific characteristics. Tab. 1 summarizes the key system parameters. The parameters in Tab. 1 are primarily sourced from the real equipment specifications. These include manufacturers' data sheets and technical manuals for solar collectors, ORC components, and other system elements. Using the real equipment data provides a realistic basis for the system modeling and analysis, ensuring that the system design reflects practical and achievable performance characteristics. The significant variations in turbine inlet and outlet pressures observed in Tab. 1 are attributed to changes in flow rates and operational conditions. These variations are critical for ensuring the reliability and efficiency of the system. The pressure values P_{3a} and P_{3b} mentioned in

Tab. 1 are absolute pressures, considering the reference pressure is defined at 101.325 kPa. Notably, the design considers Mardin province's average solar radiation of 6.0271 kWh/m^2.

Table 1. System parameters

T_{1a} **(K)**	478.15
T_{1b} **(K)**	353.15
T_{2a} **(K)**	473.15
T_{2b} **(K)**	348.15
T_{3a} **(K)**	468.15
P_{3a} **(kPa)**	3200-3000-2800-2600-2400
P_{3b} **(kPa)**	100-200-300-400-500-600-700-800-900-1000
T_{3c} **(K)**	310.15
T_{4a} **(K)**	288.15
T_{4b} **(K)**	298.15

2.1. Thermodynamic Analysis

In the thermodynamic analysis, it's imperative to establish a reference state, which is defined as 25 ºC and 101.325 kPa. Additionally, the temperature of the sun is assumed to be 4800 K, providing a crucial parameter for evaluating the system's performance. It's noteworthy that kinetic and potential energy effects are considered negligible within this analysis, streamlining the focus on other significant factors. Moreover, the efficiencies of the various units comprising the system are detailed in Tab. 2, offering essential insights into their respective contributions to overall performance. This comprehensive approach ensures a thorough examination of the system's capabilities and provides valuable data for optimization and further refinement.

Table 2. The system units' efficiencies [20,21, 23, 24, 25]

Thermal energy storage unit (η_{test})	0.98
Isentropic efficiency of turbine (η_t)	0.85
Generator (η_g)	0.99
Isentropic efficiency of pump (η_p)	0.90
Heat exchanger (η_{he})	0.98
Collector heat loss coefficient (U_L)	3.82 W/m^2 °C
Thermal conductivity of receiver (k)	16 W/m °C
Transmissivity of cover glazing (τ_c)	0.90
Effective transmissivity of PC (τ_{PC})	0.94
Absorptivity of the receiver (α_{ar})	0.87
Incidence angle modifier ($\kappa(\theta)$)	0.89
Intercept factor (γ)	0.95

2.2. Energy Analysis

The governing energy equations for the S-ORC were derived through the following procedures. The calculation of the net solar energy gained by the parabolic collector can be conducted as elaborated in [22].

$$\dot{Q}_{pc} = N.F_R.\left[I.A_a.\eta_{pc} - A_r.U_L.(T_{1b} - T_0)\right] \quad (1)$$

here, *N* represents the number of collectors, *I* denotes solar radiation, A_a represents the aperture area, T_{1b} signifies the receiver inlet temperature of the Therminol, T_0 denotes the ambient temperature. Additionally, the efficiency of the parabolic collector is also taken into account.

$$\eta_{pc} = \alpha_r . \tau_{PC} . \kappa(\theta) . \tau_{PC} \tag{2}$$

here, η_{pc} represents the efficiency of the parabolic collector. The calculation of heat transferred from the sun can be determined as follows:

$$\dot{Q}_{sun} = I . A_a . N \tag{3}$$

The mass of the terminol can be calculated as;

$$\dot{m}_1 = \frac{\dot{Q}_{pc}}{(T_{1a} - T_{1b}) . c_{terminol}} \tag{4}$$

The turbine power;

$$\dot{W}_t = \dot{m}_{wf} . (h_{3a} - h_{3b}) \tag{5}$$

The electrical power output of the generator can be calculated as;

$$\dot{W}_g = \eta_g . \dot{W}_t \tag{6}$$

The power consumption occurring in the pump;

$$\dot{W}_p = \dot{m}_3 . (h_{3d} - h_{3c}) \tag{7}$$

The heat is transferred at the heat exchanger;

$$\dot{Q}_{he} = \dot{m}_2 . (h_{3a} - h_{3b}) . \eta_{he} \tag{8}$$

The net power output;

$$\dot{W}_{net} = \dot{W}_g - \dot{W}_p \tag{9}$$

The energy efficiency of the system;

$$\eta_{S-ORC} = \frac{\dot{W}_{net}}{\dot{Q}_{sun}} \tag{10}$$

2.3. Exergy Analysis

The exergy balance equation for steady systems is provided as follows:

$$\dot{E}_{X_{heat}} - \dot{E}_{X_{work}} + \dot{E}_{X_{m,i}} - \dot{E}_{X_{m,o}} = \dot{E}_{X_{dest}} \tag{11}$$

The exergy flow (ψ) is given as:

$$\psi = (h - h_0) - T_0 . (s - s_0) \tag{12}$$

In this equation, *h* represents enthalpy, *s* denotes entropy, and the subscript zero indicates properties of fluids at the dead state. The calculation of the exergy of mass flow is conducted as follows:

$$\dot{E}_{X_m} = \sum \dot{m} . \psi \tag{13}$$

The exergy of solar radiation is determined as described in reference [23];

$$\dot{E}_{X_{sun}} = A_a . N . I . (1 + (1/3) . (T_0/T_{sun})^4 - (4/3) . (T_0/T_{sun})) \tag{14}$$

The exergy balance of the parabolic collector is computed as;

$$\dot{E}_{X_{sun}} + \dot{E}_{X_{1a}} - \dot{E}_{X_{1b}} = \dot{E}_{X_{dest,pc}} \tag{15}$$

The exergy balance of the thermal energy storage tank is determined as follows:

$$\dot{E}_{X_{1b}} + \dot{E}_{X_{2b}} - \dot{E}_{X_{1a}} - \dot{E}_{X_{2a}} = \dot{E}_{X_{dest,test}} \tag{16}$$

The exergy balance of the heat exchanger is computed as;

$$\dot{E}_{X_{2a}} + \dot{E}_{X_{3d}} - \dot{E}_{X_{2a}} - \dot{E}_{X_{3a}} = \dot{E}_{X_{dest,he}} \tag{17}$$

The exergy balance of the turbine is computed as;

$$\dot{E}_{X_{3a}} - \dot{E}_{X_{3b}} - \dot{W}_t = \dot{E}_{X_{dest,t}} \tag{18}$$

The exergy balance of the condenser is computed as;

$$\dot{E}_{X_{3b}} + \dot{E}_{X_{4a}} - \dot{E}_{X_{3c}} - \dot{E}_{X_{4b}} = \dot{E}_{X_{dest,c}} \tag{19}$$

The exergy balance of the pump is computed as;

$$\dot{E}_{X_{3c}} - \dot{E}_{X_{3d}} + \dot{W}_p = \dot{E}_{X_{dest,p}} \tag{20}$$

The exergetic efficiency of the system components is determined using the following equation:

$$\varepsilon = 1 - \frac{\dot{E}_{X_{dest,coponent}}}{\dot{E}_{X_{inlet}}} \tag{21}$$

The reference state is defined as 101.325 kPa and 293.15 K. The exergy efficiency of the system is calculated accordingly.

$$\varepsilon_{S-ORC} = \frac{\dot{W}_{net}}{\dot{E}_{X_{sun}}} \tag{22}$$

2.4. Exergoeconomic Analysis

The investment costs of the system components are determined using the Module Costing Technique [24-25]. The data utilized for calculating the purchase costs of equipment were sourced from the literature in 2001 [25]. These costs were subsequently adjusted for the year 2022 using the Chemical Engineering Plant Cost Index (CEPCI) [26]. To calculate the equipment costs for 2022, the following procedure is employed:

$$C_{eq} = \frac{CEPCI_{2022}}{CEPCI_{2001}} . F_{BM} . C^0 \tag{23}$$

here, F_{BM} represents the bare module cost factor, C^0 denotes the purchase cost of equipment, and $CEPCI_{2001}$ refers to the CEPCI in 2001, which is 397 [24]. The purchase cost of equipment is calculated using the following equation [25]:

$$log\ C^0 = K_1 + K_2 . log\ X + K_3 . (logX)^2 \tag{24}$$

here, K represents constants determined based on the equipment, and X is the parameter related to the equipment. These parameters include the heat transfer area for the heat exchanger and condenser, power consumption for the pump, and power output of the turbine. The bare module cost factors can be calculated as described in [25]:

$$F_{BM} = B_1 + B_2 . F_M . F_p \tag{25}$$

here, B represents constants based on equipment types, F_M denotes the material factor, and F_P the pressure factor. The pressure factor of the pump can be calculated using the method outlined in [25]:

$$logF_P = C_1 + C_2.log\ P_p + C_3.\left(logP_p\right)^2 \quad (26)$$

here, *Pp* represents the design pressure of the pump. The constants of the cost equations corresponding to the equipment are provided in Tab. 3.

Table 3. The constants of the cost equations [25]

Equipment	Constant										
	K_1	K_2	K_3	B_1	B_2	F_M	F_{BM}	F_P	c_1	c_2	C_3
Heat exchanger	4.6656	-0.1557	0.1547	0.9600	1.210	2.450	-	1.0000	0.0000	0.0000	0.0000
Condenser	4.6420	0.3698	0.0025	-	-	-	3.000	0.0000	0.0000	0.0000	0.0000
Turbine	2.6259	1.4398	-0.1776	-	-	-	11.600	-	-	-	-
Pump	3.3892	0.0536	0.1538	1.8900	1.350	2.200	-	-	-0.3935	0.3957	-0.0023

The investment cost of the thermal energy storage system and parabolic collector is initially estimated at 32.5$/kWh$_{th}$ [27] and 170 $/m2 [28] for the years 2013 and 2015, respectively. These costs are then adjusted for the year 2022 using the CEPCI [26]. The investment cost of the parabolic collector is taken as 32.5$/kWh. Furthermore, in systems, both mass and energy transfer can be viewed as exergy transfer. While a portion of the transferred exergy constitutes the system's output, some is inevitably lost due to irreversibility within the system. If the unit exergy price is denoted by "c", the total exergy price can be expressed by the following equation:

$$C = c.\dot{Ex} = c.m.ex \quad (27)$$

When computing the exergy cost, each component within the system is considered individually. The exergy cost balance equation for the k_{th} component of a system can be expressed as the following equation:

$$\sum C_{e,k} + C_{w,k} = C_{q,k} + \sum C_{i,k} + Z_k \quad (28)$$

here Z_k represents the Levelized monetary value, encompassing the investment, operation, and maintenance costs associated with the k_{th} component. This value (Z) is determined based on parameters such as annual operating time, system lifespan, interest rate, and escalation rate. It can be expressed by the following equation:

$$Z = A\left[\frac{Initial\ investment\ cost}{System\ Life\ x\ Annual\ Working\ Hours} + \frac{Electricity\ Expenses + Maintenance\ Expenses}{Annual\ Working\ Hours}\right] \quad (29)$$

here A denotes a Levelized value factor and can be expressed in the following equation [29];

$$A = \frac{CELF}{1+r_i} \quad (30)$$

here r_i denotes the interest ratio, *CELF* denotes the Fixed Escalation Correction Factor and is computed as:

$$CELF = \frac{k(1-k^n)}{1-k}CRF \quad (31)$$

here k denotes a value contains the Levelized Price Correction Factor, n denotes a value indicates the foreseeable lifetime for the system or system component, *CRF* represents the Capital Recovery Factor and is computed as;

$$CRF = \frac{i_{eff}(1+i_{eff})^n}{(1+i_{eff})^n-1} \quad (32)$$

here i_{eff} denotes the repayment ratio. Evaluations of a component's performance are provided by the thermoeconomic factor (exergoeconomic) defined for each component. The exergoeconomic factor for the k_{th} component of the system can be calculated as Equation 33[30].

$$f = \frac{Z}{Z + c\dot{E}x_k} \tag{33}$$

The values used in the exergoeconomic analysis of the system are given in Tab. 4. The parameters in Tab. 4 are derived from both literature sources and real-world cost data. The literature provides benchmark values and ranges for various economic factors such as initial investment costs, maintenance costs, and operational expenses. These values were supplemented with data from actual projects and market surveys to ensure that the economic analysis reflects current market conditions and realistic cost estimates.

Table 4. Values used in exergoeconomic analysis of the system

r (%)	n (year)	t (hour)	r_n	k	I_{EFF}	CRF	CELF	A
0.158	20	8400	0.04	0.981	0.06	0.087	1.436	1.241

The study utilized MATLAB, EES, REFPROP, and Microsoft Excel software. The combination of these computational platforms provided a comprehensive approach to the research. MATLAB and EES offered robust numerical computation and equation-solving capabilities essential for accurate thermodynamic and exergoeconomic analysis. REFPROP ensured precise calculation of fluid properties, enhancing the reliability of the modeling process. Microsoft Excel complemented these tools by facilitating data organization and visualization. By leveraging these platforms, the study delivered a robust and reliable analysis, offering valuable insights into the performance and economics of S-ORC systems.

3. Results and Discussions

This section provides a detailed explanation of the methodology implemented in this study, outlining the systematic approach taken to achieve the research objectives. It begins with the identification of the research problem and the establishment of the study's scope and boundaries. A thorough literature review follows, highlighting existing research on S-ORC systems and identifying gaps that this study aims to address. The system design and modeling phase includes developing a detailed model of the S-ORC system and defining the necessary parameters and assumptions. Data collection focuses on gathering relevant information specific to Mardin, Turkey, including weather, solar radiation, and economic data. The core of this section is the exergoeconomic analysis, which integrates exergy analysis to evaluate thermodynamic performance and economic analysis to assess cost-effectiveness. The results are then analyzed and discussed in comparison with existing literature, emphasizing practical applications and policy implications. The section concludes with a summary of key findings and recommendations for future research and practical implementations.

Fig. 3 illustrates the net power values obtained from energy analysis results for the S-ORC system, varying with different turbine inlet and outlet pressures. These analyses were conducted based on parabolic collectors specifically designed for Mardin Province.

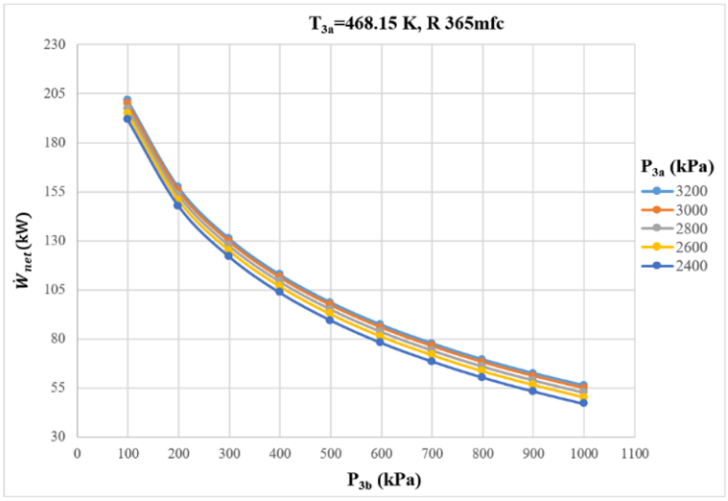

Figure 3. Net power values obtained from the system for different turbine pressures

Upon examination of Fig. 3, it is evident that the net power output varies between 46.894 kW and 201.597 kW depending on the turbine inlet and outlet pressure values. The maximum power output from the system was observed at the turbine inlet pressure of 3200 kPa and the turbine outlet pressure of 100 kPa. This significant variation in power output highlights the importance of optimizing turbine pressures to achieve maximum efficiency and performance of the ORC system. Variations in flow rates directly affect irreversibility within the system, thus influencing power output. Therefore, the relationship between power output and pressure variations has been carefully analyzed. The data suggests that careful adjustment of inlet and outlet pressures can lead to substantial improvements in power generation, making the system more effective for practical applications in Mardin Province. Fig. 4 illustrates the variation in energy efficiency of the system obtained from different system designs, as derived from the energy analysis results.

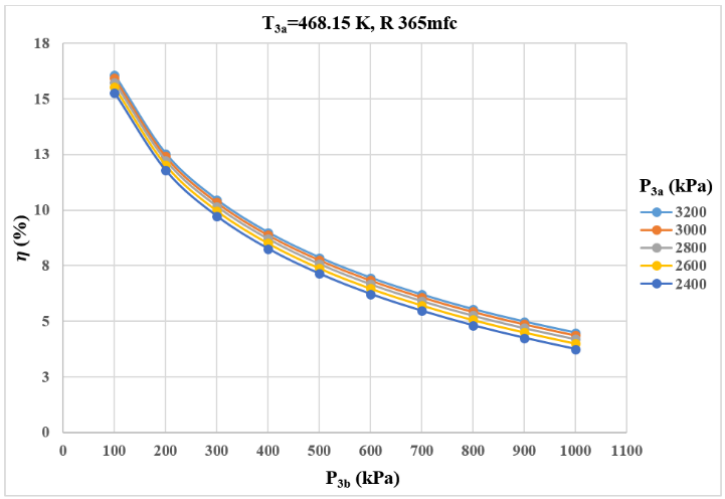

Figure 4. Variation of Energy efficiency of the system for different turbine pressures

Upon examining Fig. 4, it becomes apparent that the energy efficiency of the system fluctuates between 3.74% and 16.079%. The highest energy efficiency achieved from the system was observed in the configuration utilizing a turbine inlet pressure of 3200 kPa and a turbine outlet pressure of 100 kPa. This indicates a strong correlation between turbine pressure settings and system efficiency. The minor discrepancies (~1%) observed in efficiency values are due to inherent uncertainties in the

calculation methodology. These uncertainties have been carefully analyzed to enhance the reliability and consistency of system performance. The substantial range in efficiency values underscores the critical impact of precise pressure optimization on the overall performance of the ORC system. The data reveal that specific configurations can significantly enhance energy conversion, making the system more viable for practical use. Moreover, these findings highlight the potential for further research and development to refine these pressure settings, thereby maximizing the efficiency and sustainability of S-ORC systems in applicable regions. Fig. 5 depicts the variation in the exergy efficiency of the system across all configurations.

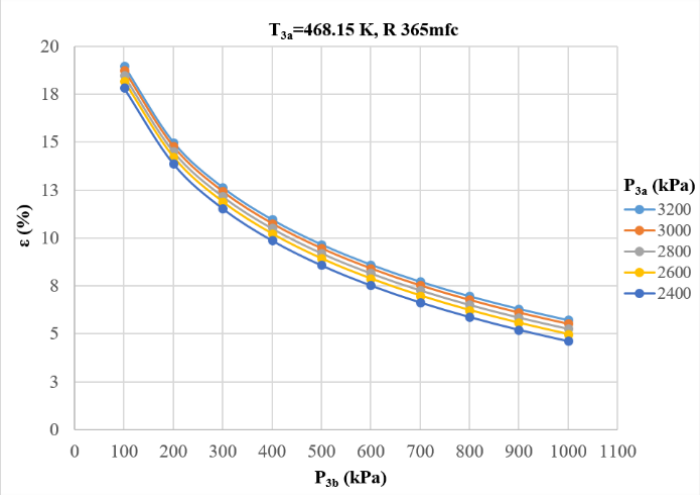

Figure 5. Variation of exergy efficiency of the system for different turbine pressures

Upon examination of Fig. 5, it is evident that the exergy efficiency of the system varies across all configurations, ranging approximately from 4.627% to 18.977%. Notably, the highest exergy efficiency was observed at the turbine inlet pressure of 3200 kPa and the turbine outlet pressure of 100 kPa, mirroring the conditions for maximum energy efficiency. This variability underscores the importance of system design and parameter optimization in achieving optimal performance. The data suggest that fine-tuning the turbine pressures can lead to significant improvements in exergy efficiency, highlighting the critical role of detailed system analysis and targeted adjustments. These findings emphasize the potential for enhanced energy conversion and greater sustainability in S-ORC systems through meticulous design and optimization efforts. Furthermore, Fig. 6 provides insights into the exergy destruction values of the components for the most efficient system configurations. This detailed analysis aids in identifying areas for potential improvement and optimization within the system design.

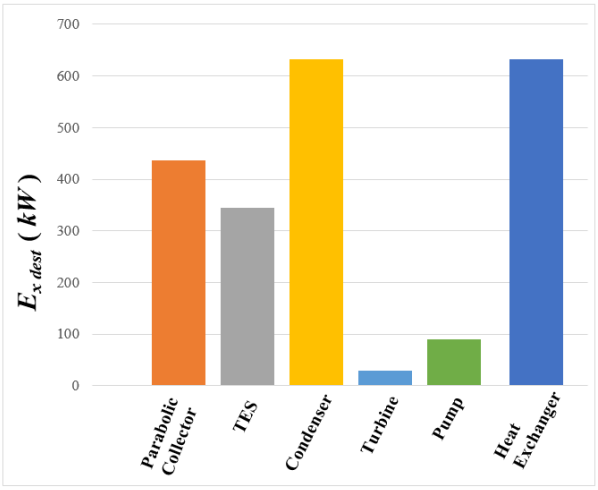

Figure 6. Exergy destruction values of system components

Upon reviewing Fig. 6, it becomes apparent that the highest exergy destruction among the system components was observed in the Heat Exchanger, totaling 632.466 kW, whereas the lowest exergy destruction was attributed to the turbine, amounting to 29.927 kW. This significant disparity in exergy destruction underscores the importance of targeting the heat exchanger for efficiency improvements. By focusing on optimizing the design and operation of the heat exchanger, it is possible to achieve substantial reductions in energy losses and enhance overall system performance. This disparity in exergy destruction emphasizes the significance of optimizing component efficiency and design to minimize energy losses within the system. Additionally, these findings suggest that even components with relatively low exergy destruction, like the turbine, can contribute to overall system efficiency if further refined. Therefore, a holistic approach to system optimization, considering both major and minor components, is essential for achieving maximum exergy efficiency. Furthermore, as a result of the exergoeconomic analysis conducted for the system, the values pertaining to the system and its individual components are provided in Tab. 5. This comprehensive analysis offers valuable insights into the economic viability and performance optimization of the system, facilitating informed decision-making and further refinement of the design.

Table 5. Values used in exergoeconomic analysis of the system

Component	**Z**	**C**	**F**	**y_{ky}(%)**
Parabolic Collector	25.293	16.163	61.012	28.437
TES	0.609	12.771	4.554	22.470
Heat exchanger	7.289	53.394	12.012	41.175
Turbine	9.186	8.416	52.185	1.948
Condenser	9.712	160.163	5.717	5.869
Pump	0.565	0.294	65.802	0.101

Upon examination of Tab. 5, it is observed that the highest Levelized total cost for the system components amounted to 25.293$/h, while the lowest Levelized total cost was attributed to the parabolic collectors at 0.565$/h for the pump. This indicates a significant variation in cost distribution among the components, highlighting the need for targeted cost optimization strategies. Additionally, the highest exergy cost value was determined for the condenser, totaling 160.163$/kW, whereas the lowest exergy cost value was associated with the pump at 0.294$/kW. These exergy cost values reflect the economic impact of inefficiencies within each component, suggesting areas where cost-effective improvements can be made. Moreover, the analysis revealed that the components with the highest

exergy loss rates in the system were the Heat Exchangers, parabolic collectors, and TES with rates of 41.175%, 28.437%, and 22.470%, respectively. These findings underscore the significance of optimizing the performance and efficiency of these components to minimize exergy losses and enhance overall system efficiency. By focusing on reducing exergy losses in the most critical areas, the overall sustainability and cost-effectiveness of the system can be significantly improved. Furthermore, Fig. 7 presents the Exergoeconomic factor values of system components across different turbine inlet and outlet pressures. This comprehensive analysis aids in understanding the economic implications of system design parameters and facilitates informed decision-making for optimizing system performance while considering economic factors.

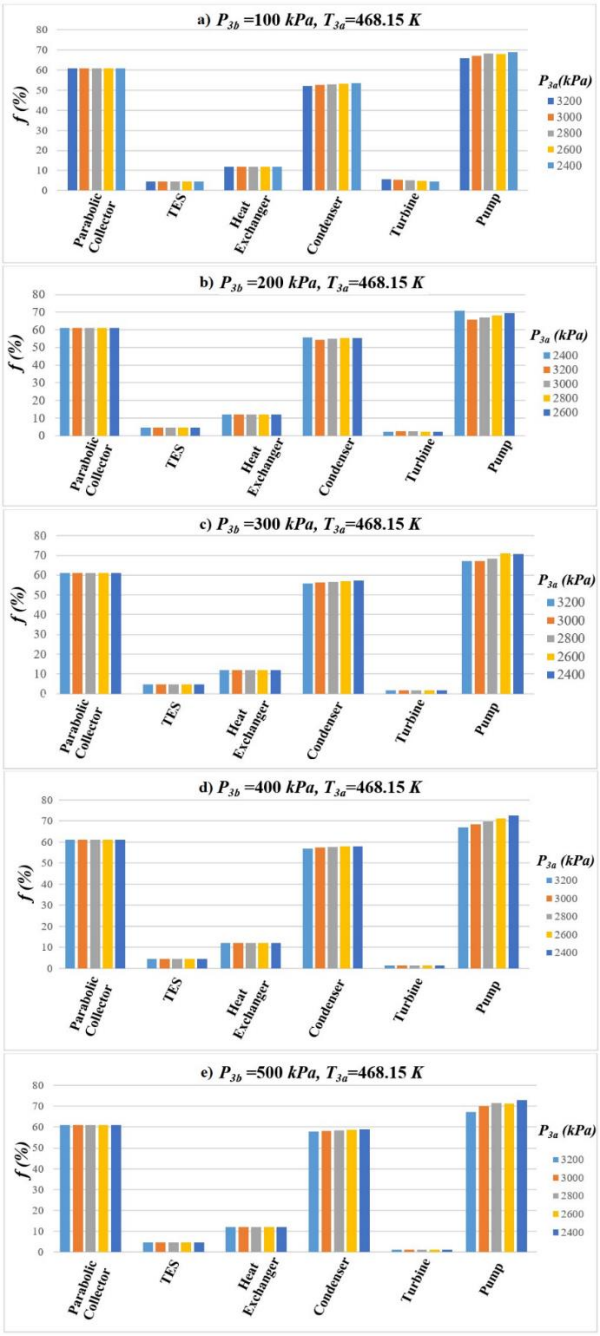

Figure 7. Exergoeconomic factor values of system components for different turbine inlet and outlet pressures (a, b, c, d, e)

Upon reviewing Fig. 7 and Tab. 5 concurrently, it becomes evident that the highest exergoeconomic factor values are attributed to the pump, parabolic collector, and condenser, respectively. This analysis highlights the substantial economic impact of certain components compared to others, emphasizing the need for a balanced approach in system design. Conversely, the lowest exergoeconomic factor values are associated with the turbine, TES, and Heat Exchanger. This comparison highlights the varying economic impacts of different system components and underscores the importance of considering both exergy and economic factors in system design and optimization processes. By identifying components with higher exergoeconomic factor values, decision-makers can prioritize optimization efforts, focusing resources on areas that will yield the most significant improvements in system efficiency and economic performance. This integrated approach ensures that both technical and economic aspects are addressed, leading to a more sustainable and cost-effective system.

4. Conclusions

In this study, the S-ORC was meticulously designed utilizing long-term solar radiation data specific to Mardin Province. Through comprehensive analysis, the net power output from the system ranged between 29.927 kW and 201.597 kW. The system's efficiency exhibited variability ranging from 3.74% to 16.079%, while the exergy efficiency spanned from 4.627% to 18.977%.

The analysis pinpointed the heat exchanger as the component with the highest exergy destruction, reaching 632.466 kW. A lower exergoeconomic factor for any system element suggests potential savings through minimizing exergy losses in that component. Conversely, a higher exergoeconomic factor indicates that the initial investment cost outweighs the exergy efficiency, warranting a focus on reducing the initial investment for that element. In this context, the components identified with the highest exergy losses in the system were the heat exchanger, parabolic collectors, and TES, respectively. This indicates a significant opportunity for optimizing these components to reduce energy losses and improve overall system efficiency. Furthermore, the analysis revealed that specific configurations of turbine pressures could lead to substantial improvements in both energy and exergy efficiencies, highlighting the critical role of precise parameter optimization in enhancing system performance. Furthermore, the pump, parabolic collectors, and turbine emerged with the highest exergoeconomic factor values, while the TES, condenser, and heat exchanger were associated with the lowest exergoeconomic factor values. This implies that while the pump and parabolic collectors require a higher initial investment relative to their exergy efficiency, there is considerable room for cost reduction and efficiency improvement in these components through targeted optimization strategies.

Based on these analyses, it is evident that a holistic approach to system optimization is essential. This includes focusing on components with high exergy destruction to minimize losses and enhance efficiency, as well as addressing economic factors to ensure cost-effectiveness. The integration of conventional systems with renewable energy sources, as demonstrated in this study, not only improves energy sustainability but also offers a viable pathway for reducing dependence on fossil fuels.

The designed system demonstrates suitability for deployment in Mardin Province and serves as a promising model for integrating conventional systems with renewable energy systems, paving the way for sustainable energy practices in the region. Future research should focus on further refining the

optimization of system parameters, exploring advanced materials and technologies for key components, and assessing the long-term economic benefits of widespread adoption of S-ORC systems in similar climatic regions.

Nomenclature

Symbols and Abbrevations

ORC	Organic Rankine Cycle
S-ORC	Solar assisted organic Rankine Cycle
TES	Thermal energy storage
$\dot{E}_X$	Exergy (kW)
ε	Exergetic efficiency
f	Exergoeconomic factor
η	Efficiency
y_{ky}	Exergy loss rate

REFERENCES

[1] Bou Lawz Ksayer, E., Design of an ORC system operating with solar heat and producing sanitary hot water, *Energy Procedia*, *6* (2011), pp.389–395, doi:10.1016/j.egypro.2011.05.045.

[2] Zhang, X.-R., Yamaguchi, H., Uneno, D., Experimental Study On The Performance Of Solar Rankine System Using Supercritical CO_2, *Renewable Energy*, *32* (2007), pp. 2617–2628, doi:10.1016/j.renene.2007.01.003

[3] Ango, A. M. D., Leveque, G., Holaind, N., Henry, G., Leroux, A., Low Temperature and Power Solar Energyconversion for Domestic Use, *Energy Procedia*, *161* (2017), pp. 454–463.

[4] Li, C., Wang, Z., Liu, H., Guo, F., Li, C., Xiu, X., Wang, C., Qin, J., Wei, L., Exergetic and Exergoeconomic Evaluation of an SOFC-Engine-ORC Hybrid Power Generation System with Methanol for Ship Application, *Fuel*, *357* (2024), pp. 1-13.

[5] Wang, X.D., Zhao, L., Wang, J.L., Zhang, W.Z., Zhao, X.Z., Wu, W., Performance Evaluation Of A Low-Temperature Solar Rankine Cycle System Utilizing R245fa, *Solar Energy*, *84* (2010), pp.353–364, doi:10.1016/j.solener.2009.11.004.

[6] Desai, N.B., Bandyopadhyay, S., Optimization of Concentrating Solar Thermal Power Plant Based On Parabolic Trough Collector, *Journal of Cleaner Production*, *89* (2015), pp.262–271. doi:10.1016/j.jclepro.2014.10.097.

[7] Zhu, J., Huang, H., Performance Analysis of a Cascaded Solar Organic Rankine Cycle with Superheating, *International Journal of Low-Carbon Technologies*, 11 (2016), pp.169–176, doi:10.1093/ijlct/ctu027.

[8] Mitrovic, D. M., Stojanovic, B. V., Janevski, J. N. Ignjatovic, M. G., Vuckovic, G. D., Exergy and Exergoeconomic Analysis of a Steam Boiler, *Thermal Science*, *22* (2018), 5, pp. 1601-1612.

[9] Marques, A. S., Benito, Y. R., Ochoa, A. A., Carvalho, M. Thermoeconomic Analysis of a Microcogeneration System Using the Theory of Exergetic Cost, *Thermal Science*, *23* (2023), 5A, pp. 3579-3589.

[10] Unal, F., Temir, G., Koten, H., Energy, Exergy and Exergoeconomic Analysis of Solar-Assisted Vertical Ground Source Heat Pump System for Heating Season, *Journal of Mechanical Science and Technology*, 32 (2018), pp. 3929-3942.

[11] Unal, F., Ozkan, D. B., Application of Exergoeconomic Analysis for Power Plants, *Thermal Science*, 22 (2018), 6 Part A, pp. 2653-2666.

[12] Unal, F., Energy and Exergy Analysis of an Industrial Corn Dryer Operated by Two Different Fuels, *International Journal of Exergy*, *34* (2021), 4, pp. 475-491.

[13] Unal, F., Temir, G., Exergo Economic Analysis of the Ground Source Heat Pump for Cooling Seasons in The Mardin Province, *Sigma Journal of Engineering and Natural Sciences*, 32 (2014), 4, 477-488.

[14] Unal, F., Akan, A. E., Demir, B., Yaman, K., 4E Analysis of an Underfloor Heating System Integrated to The Geothermal Heat Pump for Greenhouse Heating, *Turkish Journal of Agriculture and Forestry*, 46 (2022), 5, pp. 762-780.
[15] Boydak, O., Ekmekci, I., Yilmaz, M., Koten, H., Thermodynamic Investigation of Organic Rankine Cycle Energy Recovery System and Recent Studies, *Thermal Science*, 22 (2018), 6 Part A, pp. 2679-2690.
[16] Gao, G., Li, J., Cao, J., Yang, H., Pei, G., Su, Y., The Study of a Seasonal Solar CCHP System Based On Evacuated Flat-Plate Collectors and Organic Rankine Cycle, *Thermal Science*, *24* (2020), 2A, pp. 915-924.
[17] Zhao, X., Yang, S., Liu, Z., Wang, D., Du, Z., Ren, J., Optimization and Exergoeconomic Analysis of a Solar-Powered ORC-VCR-CCHP System Based On a Ternary Refrigerant Selection Model, *Energy*, *290* (2024), 129976, pp. 1-18.
[18] Quoilin, S., Orosz, M., Hemond, H., Lemort, V., Performance and Design Optimization Of A Low-Cost Solar Organic Rankine Cycle For Remote Power Generation, *Solar Energy*, *85* (2011), pp.955–966, doi:10.1016/j.solener.2011.02.010.
[19] Lemmon, E.W., Bell, I.H., Huber, M.L., McLinden, M.O., NIST Standard Reference Database 23: Reference Fluid Thermodynamic and Transport Properties-REFPROP. National Institute of Standards and Technology (NIST) 2018, Version 10.0.
[20] Senturk Acar, M. and Arslan, O., Energy and Exergy Analysis of Solar Energy-Integrated, Geothermal Energy-Powered Organic Rankine Cycle, *Journal of Thermal Analysis and Calorimetry*, *137* (2019), pp.659–666.
[21] Arslan O., Ultimate evaluation of Simav-Eynal geothermal resources: design of integrated system and its energy-exergy analysis, Ph.D. thesis, Eskisehir: Eskisehir Osmangazi University. Institute of Applied Sciences; 2008 (in Turkish).
[22] Yuksel, Y.E., Thermodynamic assessment of modified Organic Rankine Cycle integrated with parabolic trough collector for hydrogen production, *International Journal of Hydrogen Energy*, (2018) pp.5832-5841.
[23] Aydin, D., Utlu, Z., Kincay, O., Thermal Performance Analysis of a Solar Energy Sourced Latent Heat Storage, *Renewable and Sustainable Energy Reviews*, *50* (2015), pp.1213–25.
[24] Cao, L., Wang, J., Chen, L. and Dai, Y., Comprehensive Analysis and Optimization of Kalina-Flash Cycles for Low-Grade Heat Source, *Applied Thermal Engineering*, *131* (2018), pp.540-552.
[25] Turton, R., Shaeiwitz, J.A., Bhattacharyya, D. and Whiting, WB., 2018, Analysis, Synthesis, and Design of Chemical Processes. 5th ed, Upper Saddle River New Jersey: Prentice Hall, USA.
[26] CEPCI 2022, citation, https://www.toweringskills.com/financial-analysis/cost-indices/
[27] Reddy RG. Novel Molten Salts Thermal Energy Storage for Concentrating Solar Power Generation. Technical Report DE-FG36-08GO18153, University of Alabama (UA), Tuscaloosa, Alabama, USA, 2013.
[28] Parthiv Kurup and Craig S. Turchi, "Parabolic Trough Collector Cost Update for the System Advisor Model (SAM)", technical report, National Renewable Energy Laboratory, NREL/TP-6A20-65228, 2015.
[29] Temir, G., Bilge, D., Thermodynamic Analysis of a Trigeneration System, *Applied Thermal Engineering*, 25 (2004), pp.411-422.
[30] Bejan A., Tsatsaronis G, Moran M., Thermal Design and Optimization, John Wiley and Sons Inc., U.S.A., 1996.

RECEIVED DATE: 11.03.2024
DATE OF CORRECTED PAPER: 29.04.2024
DATE OF ACCEPTED PAPER: 20.07.2024.